SCIENTIFIC REPORTS

OPEN

SUBJECT AREAS:
NETWORK TOPOLOGY
PATTERN FORMATION
MORPHOGENESIS
COMPUTATIONAL MODELS

Received
17 January 2014

Accepted
28 April 2014

Published
16 May 2014

Correspondence and requests for materials should be addressed to A.M. (andreea.munteanu@crg.eu)

Design principles of stripe-forming motifs: the role of positive feedback

Andreea Munteanu[1,2], James Cotterell[1,2], Ricard V. Solé[2,3,4] & James Sharpe[1,2,4]

[1]EMBL/CRG Systems Biology Research Unit, Centre for Genomic Regulation (CRG), Dr. Aiguader 88, 08003 Barcelona, Spain, [2]Universitat Pompeu Fabra (UPF), Dr. Aiguader 88, 08003 Barcelona, Spain, [3]Santa Fe Institute, 1399 Hyde Park Road, Santa Fe, NM 87501, USA, [4]Institució Catalana de Recerca i Estudis Avancats (ICREA), Pg. Lluís Companys 23, 08010 Barcelona, Spain.

Interpreting a morphogen gradient into a single stripe of gene-expression is a fundamental unit of patterning in early embryogenesis. From both experimental data and computational studies the feed-forward motifs stand out as minimal networks capable of this patterning function. Positive feedback within gene networks has been hypothesised to enhance the sharpness and precision of gene-expression borders, however a systematic analysis has not yet been reported. Here we set out to assess this hypothesis, and find an unexpected result. The addition of positive-feedback can have different effects on two different designs of feed-forward motif– it increases the parametric robustness of one design, while being neutral or detrimental to the other. These results shed light on the abundance of the former motif and especially of mutual-inhibition positive feedback in developmental networks.

Modularity is a central principle to both systems and synthetic biology[1,2]. It implies the reduction of large gene networks to a collection of small, separable subsystems. Milo et al.[3] initiated such a collection by identifying small groups of interacting genes or *network motifs* that appear statistically overrepresented in complex biological networks. This statistical motif-extraction usually involves the structure - but not the function - of the motif. A proper modularity requires that these motifs always perform a similar function in different biological contexts[4–6]. For such an assessment, systems and synthetic biology increasingly aim to explore the biological and dynamical functions of these minimal regulatory motifs. Existing studies mostly addressed the characteristics and requirements of genetic oscillators, biological switches and low-pass filters[7–9]. As the list of well-studied motifs is growing, several questions emerge: What happens when simple modules are combined together? Does a given motif perform the same function, whether in isolation or embedded in a large network? (Fig. 1).

Here we address these questions by studying the motifs capable of performing a specific biological task. The task chosen is converting a decreasing morphogen gradient into a single stripe of gene expression. The single stripe is a key spatial feature in the early stages of the embryogenesis. It is considered a mechanistic unit in the formation and maintenance of boundaries between future tissues[10]. This scenario of an input gradient determining distinct cellular fates is referred to as positional information[11]. As a definition, a signalling molecule that generates at least two distinct cell types, or thresholds, at different concentrations is called a morphogen[12]. Examples of such threshold-controlling morphogens include Bicoid and Dorsal in *Drosophila*[13,14], activin in *Xenopus*[15] and Sonic Hedgehog in the vertebrate neural tube[16].

Initially, it was hypothesised that these thresholds are determined by different responsiveness (i.e. different number and affinity of binding sites) of the genes to the morphogen. However, recent evidence suggests that it is the regulatory logic of the developmental network itself that determines the expression patterns[14,17–20]. In other words, the response to morphogen gradients is an emergent property of the regulatory circuit rather than a property of specific genes. Together with the identification of spatiotemporal motifs from developmental gene networks[21], these observations suggest that general circuit-design principles are responsible for pattern formation at tissue level. Studying simple but essential expression patterns and the genetic circuits that produce them constitutes an approach to uncovering such principles.

From the existing studies of gene networks capable of a single-stripe pattern under a morphogen gradient, the 3-gene Incoherent Feed-Forward Motifs (IFFMs) appear as the minimal ones. These studies consisted of general computational explorations[22–24] or specific experimental implementations in synthetic and developmental biology[25–27]. More exhaustively, Cotterell & Sharpe[28] computationally analysed all 3-gene configurations and revealed that indeed the networks showing the single-stripe expression include the 3-gene IFFMs.

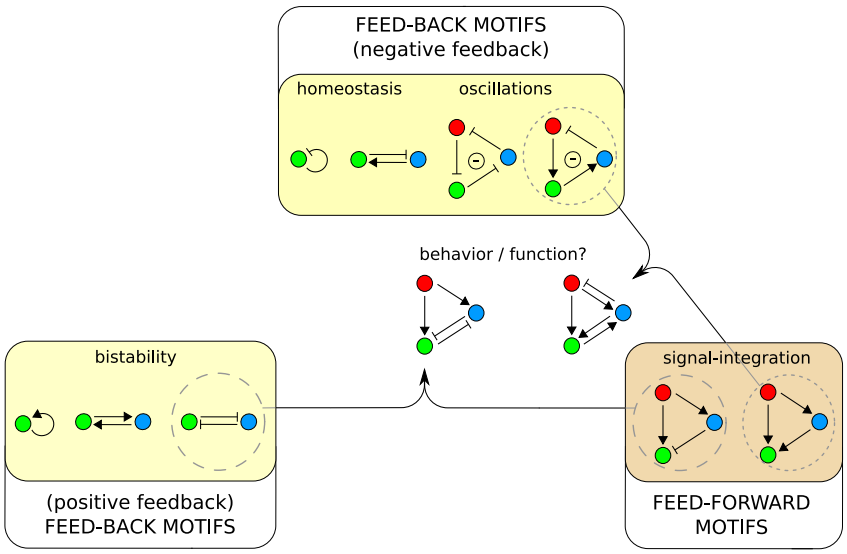

Figure 1 | Examples of functional motifs in biological networks. After identifying the biological and dynamical functions of individual network motifs, either genetic or biochemical[8], a major question still remains: will a given motif have consistent effects when added to different networks?

Beyond the mere existence of a single-stripe pattern, the sharpness and precision of this simple gene-expression pattern are crucial for the correct cell-fate specification. An unmet challenge for developmental biology is to elucidate the mechanisms that control these features and keep cell populations separated[29]. Among possible mechanisms, positive feedback within the gene network has been repeatedly hypothesised to be the primary mechanism[30–32]. Here, we set out to examine whether this hypothesis is correct, and thus assess the extent to which the positive feedback controls the formation and features of the stripe pattern. Firstly, we analytically determine the requirements and characteristics of stripe formation in IFFMs, with emphasis on developmental gene networks. Secondly, our computational exploration shows that, in spite of their similarities, the motifs respond differently to the addition of positive feedbacks. Finally, we explain this unexpected behaviour by coupling network architecture and dynamics.

Results

The model. We employ a model in which a one-dimensional tissue receives a morphogen gradient that is transformed by the cells' genetic network into a spatial pattern, here a single stripe expression in one of the genes (Fig. 2). Represented as a square, gene **A** is the only of the three genes to receive the input signal. Gene **B** is considered throughout this study as the stripe-gene, while gene **C** is the intermediate gene.

Genes integrate multiple regulations from other genes following the connectionist model[33]. This model is biologically-verified and widely-employed, especially in studying developmental gene networks[13,28,34–36] and signalling networks[8]. The regulation from gene X to gene Y is characterised by a sign (activating or inhibiting) and a weight (ω_{XY}) (see inset from Fig. 2). In the connectionist model, the effective regulating input to a gene is the sum of the weighted contributions. Finally, the rate of protein production from this gene is proportional to a saturating function of this input. We refer to this approach of summing the weighted contributions and applying a saturating filter-function as the *sum & filter* regulation model.

In endogenous tissues, proteins can diffuse between cells. However, Jaeger et al.[17] found that diffusion is not required for qualitatively generating the expression pattern of the gap genes in *Drosophila*. Cotterell & Sharpe[28] reached the same conclusion by means of an exhaustive computational study of all stripe-forming 3-gene networks. Therefore, the current study considers that proteins are non-diffusible, making our framework a positional-information scenario.

Two motifs constitute the minimal band-generators. There are four possible IFFM configurations, denoted as I_1 – I_4[7] (Fig. 3). Below each of the four minimal topologies, graphs illustrate how each motif can, or cannot, make a stripe. The upper graphs include the individual contributions from genes **A** and **C** to gene **B**, under increasing morphogen input, M. The sum of the two contributions constitutes the effective input into gene **B**. This effective input is transformed into the output (lower graphs) by the sigmoidal regulation function and time integration (see **Methods** section).

These graphs reveal two main aspects of the signal integration in IFFMs. Firstly, symmetry is observed in the signal integration for the stripe-forming I_1 and I_3 motifs: the two contributions to **B** are symmetric with respect to the morphogen axis. The symmetry stems from the topology of the two paths from morphogen to stripe gene: direct positive & indirect negative in I_1, and indirect positive and direct negative in I_3 (see **Supporting Information**, Fig. S1).

Secondly, the signal integration for the I_2 and I_4 motifs sheds light on the patterning capabilities of these motifs. I_2 has only negative interactions. According to the connectionnist model, these negative inputs are transformed into low activity from the promoter, as the promoters are considered to be non-constitutive. In other words, the I_2 motif is able to show at most a barely-detectable stripe.

A few comments on the behavior of I_2 are in order. The current study builds upon the results and accordingly borrows the connectionist framework of Cotterell & Sharpe[28] who identified the stripe-forming 3-gene networks and classified them into categories characterized by a common dynamical mechanism. In spite of the generalities of the model, a few assumptions are worth noting for their effect upon the conclusions. In the absence of external activators, self-activation can compensate for the lack of constitutive genes. From this perspective, a non-constitutive 3-link I_2 network can not produce a stripe in the absence of self-activations. In other words, a constitutive 3-link I_2 or equivalently a non-constitutive 5-link I_2 (Fig. 3) can show a pronounced single stripe of gene expression.

Finally, among the four IFFMs, the I_4 motif stands out as the only motif that cannot show a stripe under the current non-constitutive sum & filter approach. We qualitatively show this feature in Figure 3, while **Supporting Information** includes the detailed analytical proof. From these results together with the observation of low output from

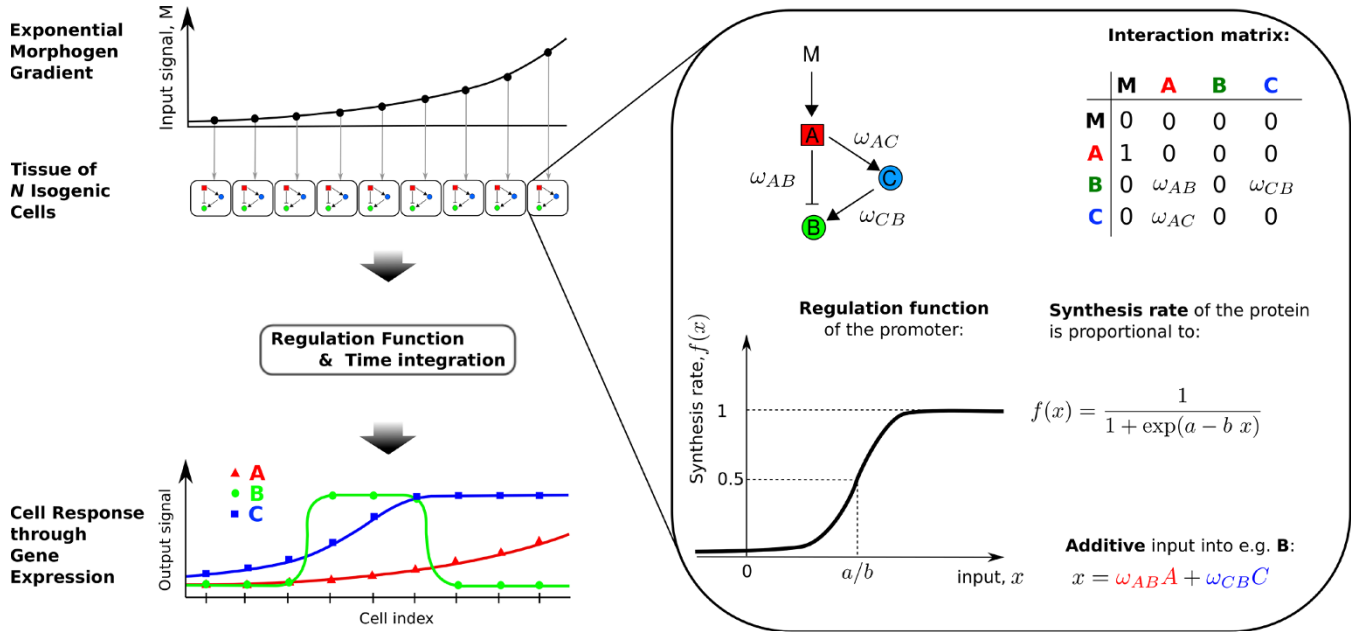

Figure 2 | The framework of the current study. An example of single-stripe formation in the positional-information scenario: the concentration of a morphogen *M* is monotonically increasing along a one-dimensional "tissue" of N isogenic cells. The underlying genetic network transforms the increasing input into a single stripe in the expression of one of the genes. Each transcription factor *X* acting at the promoter region of gene *Y* has an effect on gene expression characterised by the interaction strength ω_{XY} (*Interaction matrix*). The activating interactions have $\omega_{XY} > 0$ and inhibiting interactions, $\omega_{XY} < 0$. For each gene, the contributions from multiple transcription factors affecting it are subsequently *summed*. The resultant transcription rate from the promoter is proportional to the sigmoidal-filtering of this total contribution. The parameters *a* and *b* of the sigmoidal function *f*(*x*) control the steepness and location of the threshold value of the regulation function. The morphogen *M* is considered to be received only by gene **A** (see also **Methods** section).

I_2 network, we conclude that only I_1 and I_3 are core topologies for single-stripe formation.

Quantitatively, we also obtained analytical approximations of the factors controlling the location and width of the single stripe in IFFMs (**Supporting Information**, Fig. S2). Firstly, the *existence* of the peak is conditioned by a balance between the strengths of the activating and the inhibiting path into gene **B**. The required balance of weights is modulated by the protein degradation rate and the steepness of the regulation function (Eq. (7) in the electronic supplementary material). Secondly, the *location* of the peak is uniquely controlled by the weight of the intermediate interaction, ω_{AC}. This weight is drastically limited to low values. This ensures the positioning of the stripe within the one-dimensional tissue, as high values of ω_{AC} locate the peak outside the posterior end of the 'tissue'. Additionally, the positive contribution to **B** has an upper limit as well, as it determines the width of the stripe. It is ω_{AB} in I_1 and ω_{CB} in I_3. In both motifs, the negative interaction (ω_{CB} in I_1 and ω_{AB} in I_3) is not intrinsically restricted, being limited only with respect to the positive interactions. This relative restriction stems from the sum & filter regulation: promoters respond actively only in the presence of activators, whose effect is diminished or entirely cancelled by inhibitors. Numerical simulations reflect that indeed the positive interactions are limited to low parameter values while the negative ones have no upper limit (**Supporting Information**, Fig. S3).

Thus, we have found the parametric requirements for the *two* minimal gene-networks to transform a monotonically distributed input signal into a band-like expression in one of its constituent genes. These motifs achieve the patterning task in a symmetric and similar manner. Subsequently, we inquired into the effect of positive feedback in these alternative designs of stripe formation.

Constructing a topology-atlas by adding positive feedback. To assess the effect of positive feedback on the stripe formation, we studied a class of motifs that we refer to as RIFFMs: Reinforced Incoherent Feed-Forward Motifs. This collection (Fig. 3) constitutes the motifs based on IFFMs with all possible combinations of positive feedbacks added on and between the two downstream genes **B** and **C**. No feedback to gene **A** in these motifs would conserve the feed-forward nature of the signal.

The representation of functional I_1- and I_3-based RIFFMs (Fig. 3) recalls two 3-dimensional cubes whose nodes are the RIFFMs, and whose edges are the topological changes generating positive feedbacks. There are three types of edges associated to the addition of positive feedback. Two of them are direct positive-feedbacks: self-activation of gene **B** (dotted edges) and of gene **C** (solid edges). The third type is an indirect positive feedback formed by adding **B**-**C** interaction (dashed edges). In the case of I_1, this must be a double-negative, while in I_3, it is a double-positive.

To inquire which among the added interactions are beneficial, detrimental or neutral with respect to the interpretation of the morphogen gradient into a single stripe, we numerically determined the functional parameter space and the characteristics of the resultant stripes for all RIFFMs. Details on the definition of stripe are found in **Methods**. Figure 4 summarises the effects in terms of parameter-space extension brought by the additional interactions. This figure is a schematic, qualitative representation of the full quantitative, numerical calculations of all motifs included in Figures S4, S5 of **Supporting Information**. The graphs in Figure 4 show the comparisons performed between neighbouring RIFFMs (i.e. networks connected by one edge in the cube-representation from Fig. 3). For each branch (I_1 and I_3) we have illustrated the methodology of this comparison by chosing one of the three possible new feedbacks, and indicating (qualitatively) how the size and position of the functional parameter space (red region) changes as the new regulatory link is gradually added to the network (lower part of 4). In both cases we have chosen the indirect feedback case – ie. the feedback between B and C (the mutual repression for I_1, and the mutual activation for I_3). These examples show that the functional region in (ω_{AB}, ω_{AC}, ω_{CB})

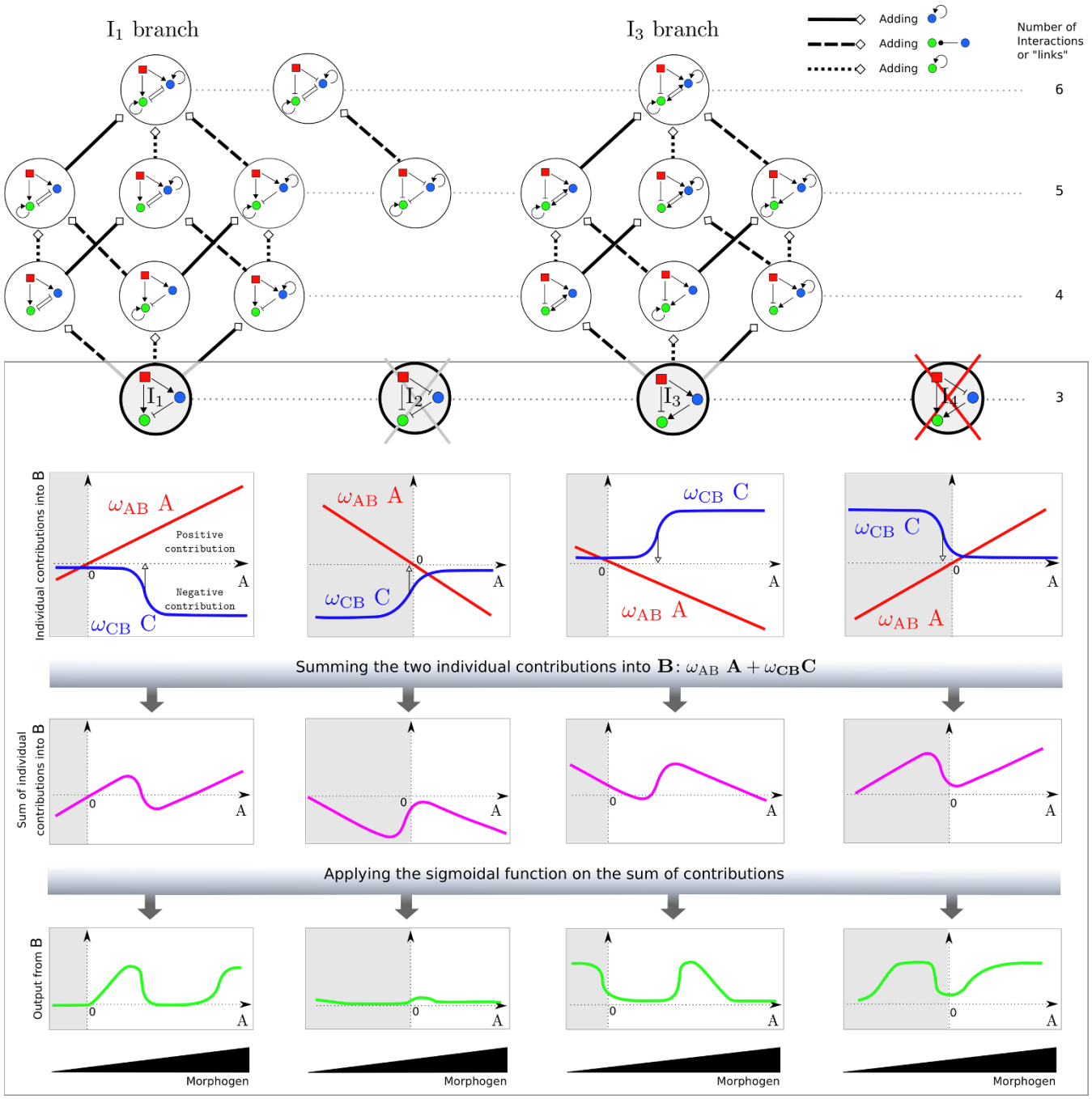

Figure 3 | The formation of the single-stripe pattern by 3-gene networks based on the four Incoherent Feed-Forward Motifs. The upper part of the figure shows the stripe-forming IFFMs reinforced with positive feedbacks, having from 4 to 6 interactions. Only interactions that generate positive feedbacks have been included. Within the I_1 and I_3 branches of stripe-forming networks, thick solid-line arrows imply adding **C** self-activation, the dashed-line arrows, **B** self-activation, and the dotted-line arrows, mutual-interaction (i.e. mutual-inhibition or mutual-activation). The lower rectangle in the figure includes the four IFFMs and the underlying process of stripe formation. It shows the generic stripes of the I_1 and I_3 networks, the lack of stripe for I_4 and the barely-detectable one for I_2. Within the rectangle, the upper graphs single out the individual contributions into the stripe-gene promoter for an increasing morphogen, *M*: from gene **A** in red, and from gene **C** in blue. For simplicity, we chose to use the concentration of *A* for the horizontal axis, instead the morphogen concentration. The lower graphs show the resultant expression from gene **B**. The Gray areas represent non-biological negative values for the concentration *A* and conceptually illustrate that I_4 would require a negative concentration of *A* to show a stripe. The range of (non-biological) negative concentration for protein *A* is also included for illustrative purposes.

expands when adding the **B**-**C** inhibition to I_1, and remains completely unchanged when adding **B**-**C** activation to I_3. In other words, the latter behavior implies that any functional set of (ω_{AB}, ω_{AC}, ω_{CB}) will maintain its functionality when the **B**-**C** activation is added. The examples in the lower part of Figure 4 compare only two 3-link networks to one of their 4-link neighbours. The full analysis schematically summarised in the upper graphs of Figure 4 consists in the comparison of the functional parameter space of all relevant motifs from one level of the atlas (i.e. *n*-link networks, with *n* being 3, 4 or 5) to the level above (i.e. (n + 1)-link networks).

We found that within each branch all these comparisons qualitatively group into three classes that directly relate to the three types of

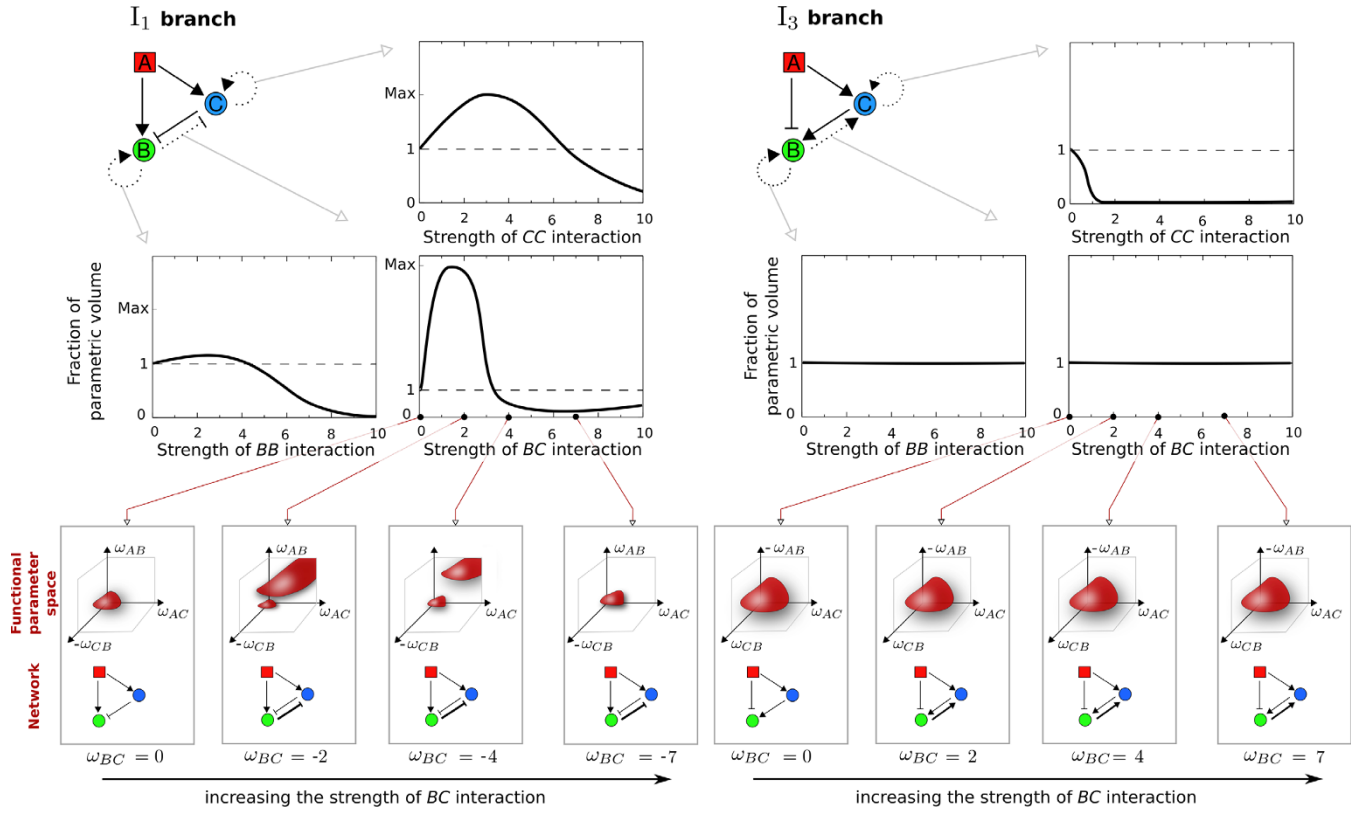

Figure 4 | Changes in the functional parameter space produced by adding positive feedbacks to the IFFMs. The positive feedbacks added to the IFFMS are: two self-activations (of gene **B** and **C**), and the **B-C** interaction. We show thus three graphs associated to these three added positive feedbacks. The graphs illustrate the change in the extent of the functional parameter space as the positive feedback increases. More precisely, they include the fraction of the functional parameter space of the RIFFMs, each scaled to the extension of the functional parameter space of a lower level RIFFM. This comparison methodology is illustrated in the lower panels for the mutual-inhibition and the mutual-activation of the 4-link networks. In these two examples, the parameter space to be compared is (ω_{AB}, ω_{AC}, ω_{CB}) with (absolute) values $\omega_{XY} \in [0, 10]$ (Gray cube). The functional region of parameter space is represented by the red shape. The behaviour illustrated in these three graphs is *generic* for the addition of each of the three types of positive feedback, independent of the existing positive feedbacks in the network. We wish to point out the parametric boost brought by the mutual-inhibition in the I_1 branch, and the complete neutrality introduced by the mutual-activation and stripe-gene self-activation in the I_3 branch.

added interactions: **B** self-activation and **C** self-activation, and the **B-C** interaction (**Supporting Information**, Fig. S4, S5). The qualitative classification of behaviours is illustrated in the three upper graphs in Figure 4. This qualitative grouping of comparisons into three classes implies that the addition of an interaction generating positive feedback has a similar effect when introduced either to a 3-link, to a 4-link or to a 5-link network, in the same branch. In other words, for a given motif, the effect of adding positive-feedback is independent on the existing interactions. We thus say the positive feedback is modular *within* a motif. In contrast to this similarity within a motif, Figure 4 reflects that positive feedback has fundamentally distinct effects in the two branches, I_1 and I_3. We thus say that the same positive feedback is non-modular *between* different motifs. In the following we discuss in more details these non-modular differences.

Parametric-boost of the I_1 design upon addition of positive feedback. In the I_1 branch, as the strength of each additional feedback interaction is gradually increased, the functional parameter space firts grows in size until it reaches a maximum and then declines. Regarding the pattern itself, within the entire branch of networks, introducing and increasing **B** self-activation widens and sharpens the single stripe pattern. Introducing and increasing **C** self-activation has an effect primarily on the right border of the stripe, displacing it posteriorly. In other words, strong values for self-activations shrink the functional parameter space.

Most interestingly, the highest parametric boost was found to occur for the creation of the mutual-inhibition module, i.e. by the addition of the **B-C** inhibition. This boost is observed at any level of the topology atlas (i.e. it is equally observed whether or not the **B** and **C** self-activations exist). In other words, for any motif in the I_1 branch with less than 6 interactions, the addition of the **B-C** inhibition enriches the functional space with parameter sets that were not functional in the absence of this interaction. While a small amount of functional parameters is lost with the addition of this interaction, significantly more parameter sets are added, producing thus a net gain of functional parameter space. Effectively, the functional region shifts in parameter space, as well as growing.

The decrease in the fraction of parametric volume for the I_1 branch beyond $|\omega_{BC}| \gtrsim 4$ in Figure 4 is a consequence of the limitation of the parameter space to the arbitrarily-chosen interval $\omega_{XY} \in [-10, 10]$. For $|\omega_{BC}| \gtrsim 4$, the stripe formation requires positive-interaction values higher than the $\omega_{Max} = 10$ considered in the numerical study. Consequently, this decrease in the functional parameter space is not an intrinsic stripe-formation restriction (**Supporting Information**, Fig. S6). This observation emphasises the fact that indeed mutual-inhibition intrinsically expands the functional parameter space at any level (i.e. to a 3-link, 4-link or 5-link motif) it is introduced within the I_1 branch.

Parametric-invariance of the I_3 design upon addition of positive feedback. Fundamentally different from the I_1 branch, the I_3 branch

shows complete neutrality for all interactions except the self-activation of (intermediate) gene **C**, for which it shows fragility (Fig. 4). By neutrality we mean that parameters sets which are functional in the absence of **B** self-activation and/or **B**-**C** activation will remain functional when these interactions are added. Added separately or simultaneously, these two interactions widen the existing stripe and sharpen its borders. Consequently, the functional parameter space of I_3 does not expand under the addition of positive feedback (see also **Supporting Information**, Fig. S7).

As in the case of I_1 branch, the addition of each interaction separately is modular within the branch. For example, the addition of **C** self-activation shows the same detrimental effect within the entire branch (i.e. either introduced at level 3 or at level 5), following the behaviour illustrated in the upper right corner of Figure 4.

Network topology drives the dynamical response to node-reinforcement. There are clear similarities between the I_1 and the I_3: they interpret the morphogen gradient into a single-stripe pattern under similar parameter conditions, display similar topological complexity, and operate in a symmetrical manner. Given these similarities, one might have expected modularity *between* these two branches (in addition to the modularity seen *within* the branches). Consequently, we sought a mechanistic explanation of these intriguing results, mainly of the parametric boost in the I_1 branch and the neutrality in the I_3 branch.

We found the explanation to be twofold. Firstly, the parametric boost brought by **B**-**C** inhibition in I_1 branch can be traced back to the sum & filter modelling approach. We have established above that a strong restriction exists for ω_{AC} in functional I_1 IFFM. High values of ω_{AC} push the stripe's center outside the limits of the 'tissue', resulting into the loss of stripe. When mutual-inhibition exists, **C** receives an activation and an inhibition that can compensate each other and achieve the functional input value to gene **C** (i.e. $\omega_{AC}A + \omega_{BC}B$). In other words, ω_{AC} can now acquire a wider set of values, as it will be compensated or reduced by **B**-**C** inhibition. This wider set of values is responsible for the parametric boost produced by the addition of **B**-**C** inhibition.

However, this compensating-interactions reasoning does not account for the neutrality present in the I_3 branch. On the contrary, fragility would be expected instead. In consequence and as the second part of the mechanistic explanation, we analysed the observed behaviour from the dynamic systems perspective. In the following, we briefly define several useful concepts from dynamic-systems theory, such as attractors, phase-portraits and nullclines.

The expectation that single-stripe formation should benefit from the addition of positive feedbacks stems from the conferred multistability, i.e. co-existence of multiple stable steady states[30,31]. A steady state is a specific value of the system's variables (here the concentrations *A*, *B*, *C*) that is indefinitely maintained by the system, in the absence of perturbations. Such a state is said to be *stable* if, under small perturbations, the system returns to this steady state; and it said to be *unstable*, otherwise. The stable steady states, or in short attractors, define distinct cell fates, a view proposed more than 60 years ago that has received recent confirmation[37]. In a multistable system, the switching from one attractor to another can act as an effective mechanism for sharp-boundary generation in the early developmental stages[30]. The attractor-switching process in itself generates two regions with distinct identities, conferred by distinct attractors, constituting the ideal mechanism for the separation of body segments and tissues.

In the current study, the lack of positive feedback in the four IFFMs implies the existence of a sole attractor (Eq. (1) in **Supporting Information**). Therefore, the stripe shape is the result of the attractor increasing and subsequently decreasing its *B*-value in response to the input signal. In other words, IFFMs' stripe has borders due exclusively to the movement of this sole attractor in phase space. The borders of this stripe are generically smooth and shallow. By containing positive feedbacks, RIFFMs can show multistability. In this case, in addition to moving the steady states, the change in morphogen concentration along the tissue also results in the destruction or creation of new steady states. By this change, RIFFMs show a qualitatively new type of stripe for which one or both borders are formed by switching between two co-existing attractors. As a representative example, the study by Manu et al.[36] concerning the stripe formation by the gap genes in *Drosophila* is the first to make the distinction between gene-expression borders formed by attractor-movement or by attractor-switching.

To exemplify these concepts, Figure 5 shows the generic stripe produced by adding mutual-interaction to I_1 and I_3. A graphical tool for determining the steady states is drawing the system's nullclines in the state space, here the space of the protein concentrations *B* and *C*. The *nullclines* are defined as the curves whose points are characterised by one variable not changing in time, i.e. the *B*-nullcline contains all those points for which the system will maintain *B* constant. One can have an intuitive understanding of the dynamics of the system from looking at the 2-dimensional (*B*, *C*) subspace instead of the full 3-dimensional (*A*, *B*, *C*) space. In such a simplified visualisation (upper and lower graphs in Fig. 5), *A* is considered to be at steady state, rapidly following the morphogen gradient. This simplification is allowed by the feed-forward nature of the RIFFMs. This 2D simplification only serves for a qualitative understanding of the typical behaviour of a RIFFM, as the timecourse of a specific parameter set requires the study of the 3D system. Employing this 2D space, we studied the change in shape and position of the nullclines produced by the change in the morphogen concentration, and the consequences on the associated steady states and thus stripe formation (see also **Supporting Information**, Movies M1–M4).

We found the *shape* of the nullclines to be determined exclusively by the interaction strengths, ω_{XY}, while the *position* of the nullcline in the (*C*, *B*) space is essentially controlled by the morphogen gradient (electronic supplementary material). More precisely, the change in morphogen concentration leads to a simple horizontal or vertical shift of the nullclines, as depicted by the red arrows in the anterior (*C*, *B*) graphs in Figure 5. The shift of nullclines creates and annihilates steady states. The simple nature of this shift provides a mechanistic perspective on the creation, destruction and selection of attractors, and the use of these events by the stripe-formation process.

The examples in Figure 5 constitute the *generic* response of the two motifs, I_1 and I_3, to the addition of mutual-interaction positive feedback. There, a non-functional parameter set for I_1 IFFM becomes functional with the addition of **B**-**C** inhibition, leading to a sharp band (middle panels). Instead, the addition of **B**-**C** activation to the I_3 IFFM sharpens a stripe already present in the IFFM.

Finally, we turn to the explanation of the neutrality in the I_3 branch. As exemplified in Figure 5, the addition of **B**-**C** activation to the I_3 IFFM changes the shape of the blue *C*-nullcline from a simple vertical curve to a sigmoidal. This transformation allows for multiple steady states, with the attractors generally located on the / diagonal in the (*C*, *B*) space. The stronger the interaction, the steeper the *C*-nullcline. Nevertheless, this steepness simply translates into a rapid attractor-movement for the left border, and a sharp attractor-switching for the right border of the stripe. In other words, this configuration of attractors allows an unlimited increase in the **B**-**C** interaction. Similarly, **Supporting Information** Figure S8 shows how the nullclines' configuration allows for full neutrality of the single-stripe pattern to the addition of **B** self-activation.

In the I_1 branch as well, the addition of **B**-**C** inhibition changes the shape of the blue *C*-nullcline from a simple vertical curve to a sigmoidal. However, the attractors are now located on the \ diagonal in the (*C*, *B*) space, instead of the / diagonal. This nullclines' configuration favours the attractor-switching for both borders. Small values of

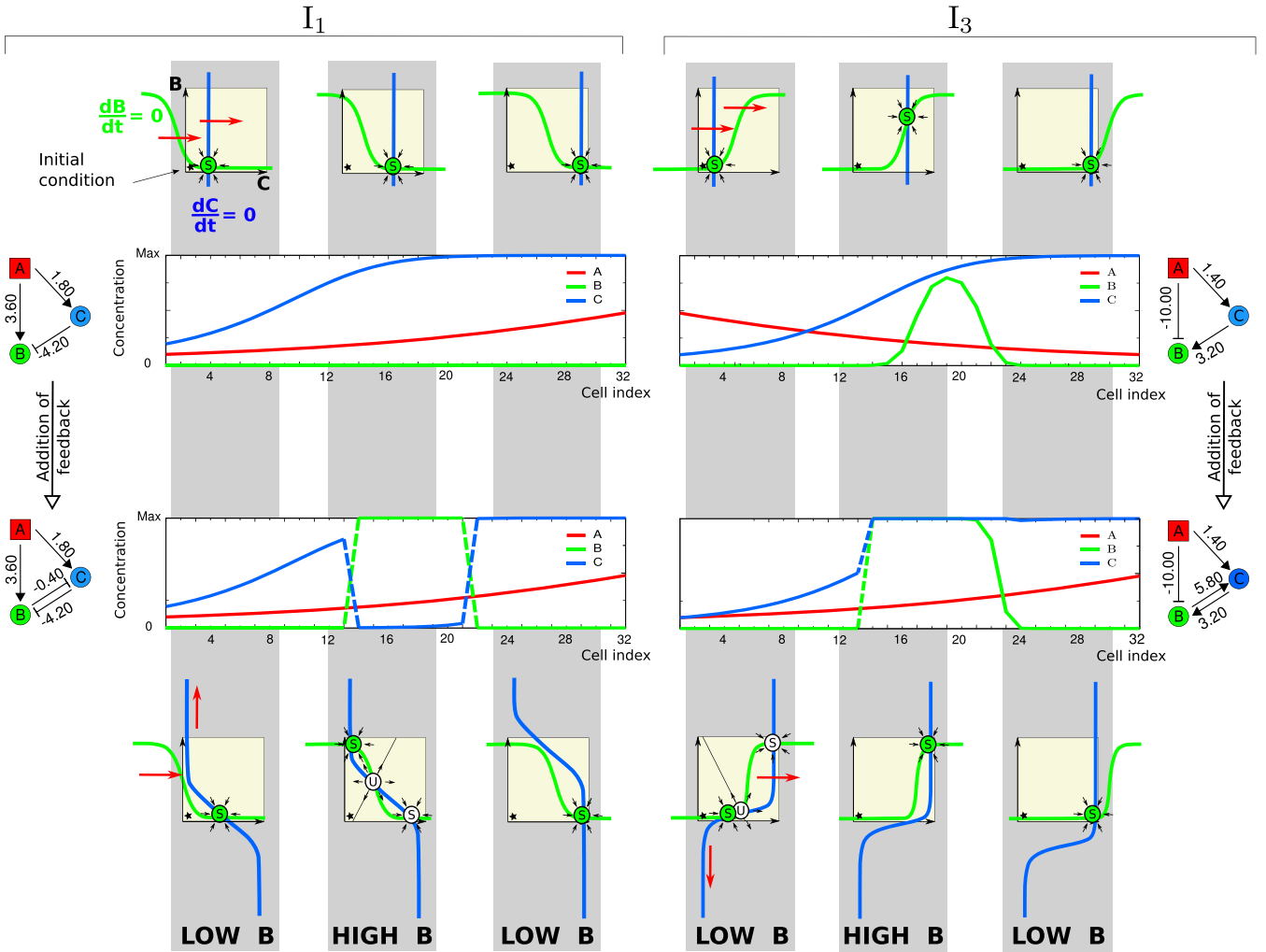

Figure 5 | Parametric boost versus neutrality: a mechanistic view. The figure illustrates the *generic* consequences of introducing **B-C** interaction leading to indirect positive feedback. Middle panels show the stripe (or lack of it) in the pure IFFMs and in the corresponding IFFM reinforced with the mutual-interaction. The dotted lines in the stripes represent attractor-switching, while the solid lines follow the attractor's movement. The Gray vertical bands qualitatively indicate the three regions, Low-High-Low, constituting the stripe in gene **B**. The yellow-background square panels are (*C*, *B*) phase plots *generically* corresponding to the three regions. There, the steady states (stable, *S* or unstable, *U*) are the intersections of nullcline curves (where one variable does not change in time – notation in the upper left corner). The black star indicates the initial condition close to the origin. The red arrows in these phase plots show that the nullclines move only horizontally or vertically in response to the morphogen gradient. When creating mutual inhibition, even a weak **B-C** inhibition allows single-stripe formation through attractor-switching process. When creating mutual activation, any value of **B-C** activation sharpens the stripe that already exists, and allows attractor-switching in the posterior border. The thin line passing through the unstable state shows the separatrix, delimiting the basins of attraction for the two stable states.

B-C inhibition are sufficient to allow for the multistability configuration prone to stripe formation.

In summary, the nullclines of the 2D simplified system act as dynamical building blocks for the generation of the stripe (see **Supporting Information**, Fig. S9 for a level-6 example). The strength of the interactions in the 3-gene system determines the shape of the nullclines, ranging from a straight line to a S-shaped sigmoidal. The change in morphogen concentration translates into a simple shift of these nullclines, affecting the existence and accessibility of attractors. The topology of the network, through the sign of the interactions, determines the orientation of the nullclines and the direction of their shift.

Discussion

We have characterised analytically and numerically the interpretation of morphogen gradient into a single-stripe of gene expression by network motifs based on two Incoherent Feed-Forward Motifs (IFFMs). Clear similarities were identified in the stripe-formation mechanism of the two IFFMs. In contrast, adding positive feedbacks to these two motifs generates different and counter-intuitive responses. These differences can be summarised as follows. Firstly, the effect of the added interaction is independent of which positive feedback-loops already exist, i.e. the addition of these positive feedbacks is modular within a motif. By contrast, the same positive feedback added to the two different motifs has different consequences on the stripe formation, i.e. the addition is non-modular between the motifs.

Secondly, the addition of positive feedbacks is beneficial for the I_1 motif (the beneficial-stripe motif), while it is neutral for the I_3 (the neutral-stripe motif). We traced the cause of neutrality to the dynamics conferred by the topology of the network motif. The phase-space reflects how the dynamics allows the I_1 motif to maintain the stripe for any strength of the added positive feedback. Conversely, the dynamics associated to the I_3 motif opens up new functional parameter regions, and thus provides parametric robustness.

Considering the IFFMs as single-stripe motifs, and the positive-feedbacks as border-sharpening motifs, the non-modular nature of their combination requires discussion. Recent studies have begun to hint towards the fragility of the dynamic-modularity assumption and the 'undesired' functional aspects of the cross-talks between motifs. For example, Ishihara & Shibata[38] show that combining (single-stripe) IFFMs into large networks gives rise to a new phenotype, the multi-stripe pattern. Complementary to the computational nature of systems biology, the approach used by synthetic biology is empirical. Synthetic biology aims at building simple genetic circuits, and ultimately at assembling these well-characterised biobricks into intricate, customisable systems. Obtaining such reliable, complex gene circuits has proved to be more challenging than expected[39]. While modularity would be undeniably useful in synthetic biology, as it is in electronic circuits, it is still not clear to what extent complex biological networks can indeed be broken down into functional motifs. It has been argued that the existence or lack of such property might reflect different evolutionary conditions[40,41]. Nevertheless, the obstacles found in the straightforward scalability of modules reveal the necessity for further exploration of network dynamics, from simple motifs up to more complex networks.

As the third and final result, the addition of the mutual-inhibition module stands out among all positive feedbacks by showing the largest expansion of the parameter space among all motifs studied. Moreover, these newly available parameter sets lead to high-expression single-stripe patterns with sharp borders, making them ideal for developmental patterning. Indeed, mutual-inhibition is a widely-employed pattern-formation motif in developmental gene networks[6,10,12]. Other computational studies pin-point the numerous biological features the mutual-inhibition module brings about, especially the increase in sharpness and precision of pattern's borders[22,26,42–45]. All these observations suggest that the mutual-inhibition module truly defines a basic design principle.

The IFFMs have been extensively studied for the variety of biological functions they perform: time-dependent and dose-dependent biphasic response[7,46,47], fold-change detection[48], optimal information processing[49] and noise buffering[50]. Among the four possible IFFMs, architectures based on I_1 are the most abundant ones in bacteria and yeast[51], a fact hypothesised to be due to its time-dependent characteristics of the IFFM. Additionally, far more I_1-based motifs than I_3 have been reported for translating morphogen gradients into single-stripe expression patterns. As well-established examples we mention the triplets activin-Xbra-Gsc[15,26], Bicoid-(knirps,Krüppel)-hunchback[52], Dorsal-(vein, rhomboid, sog)-Snail[53], EGFR-Broad-Pointed[54]. We are drawn into speculating that this abundance might in fact be because the I_1 motif is commonly forming part of a mutual-inhibition motif, even if the second reressive interaction may have been missed in many cases. For the case of the activin-Xbra-Gsc, the mutual-inhibition has been indeed confirmed[26].

With respect to the general approach of our study, a few caveats are in order. For describing the integration of different transcription factors at promoter level we employed the sum & filter formalism. The choice of the formalism determine the types of topologies revealed by the subsequent analysis. For example, the I_2 motif (Fig. 2) could become a functional stripe-maker by changing to a constitutive promoter, an additional constant activator or alternatively a pronounced self-activation of the downstream genes. Under a different framework, such as filter & multiply[22] or a more general Hill-like formalism[24], even the pure I_4 could show stripe formation due to the constitutive and AND-like features of the regulation function. However, we chose to restrict to the current formalism given the wide-spread use of the sum & filter formalism in developmental biology, and in view of existing works on stripe-forming dynamical mechanisms[28].

Still within developmental biology, the biphasic dose-dependent behaviour addressed here under the term "single-stripe formation" relates to the positional-information mechanism. By this mechanism, cells directly read and thus interpret morphogen concentration-gradients leading to their subsequent differentiation in the early developmental stages. While there is now clear evidence that patterning by morphogens is more complicated than previously thought[55,56], our goal here was the understanding of minimal regulatory motifs with the aim of elucidating the mechanistic issues and underlying design principles of this patterning process. Experimental and computational studies alike continuously emphasise the extent to which the developmental program uses such functional motifs[6,21,57,58]. In other words, these observations support the hypothesis of design principles that conceives morphogenesis in terms of decomposable functional parts carefully assembled by evolution.

However, a central question still remains, and that is why a specific network-design is chosen during evolution, when alternative designs yield similar outcomes. The work of Cağatay et al.[59] is an iconic answer to this question, showing that the topology of a genetic regulatory circuit affects its noise characteristics, as networks with identical deterministic outcomes can have profoundly different behaviours when noise is taken into account. In the current patterning context, Rodrigo & Elena[24] perform a first comparison of stripe-forming IFFMs with respect to their noise response, showing that the four IFFMs are equally good at forming narrow stripes. Among all IFFMs reinforced with positive feedbacks, only the mutual-inhibition has been thoroughly studied and found to enhance the robustness of gene-expression boundaries against variations in morphogen levels[44,45]. However, a detailed analysis and comparison of the noise response in IFFMs reinforced with positive feedbacks has not been performed yet. For discussion purposes, we performed a preliminary comparison between stripe-forming mutual-inhibition and mutual-activation modules. It reveals once more the robustness of the mutual-inhibition module: while mutual-inhibition reliably maintains the stripe borders in spite of large fluctuations, mutual-activation shows a rapid shift or even loss of the posterior border (**Supporting Information**, Fig. S10). As suggested by other studies[60], we believe this noise robustness may indeed be related to the parameter robustness revealed here in our study. In the light of all these observations, we consider a thorough stochastic analysis of all reinforced IFFMs as the logic and necessary future work that could explain the abundance of certain patterning designs in nature.

Methods

Simulation model. The parameters employed in the numerical simulations coincide with those from Cotterell & Sharpe[28] (electronic supplementary material): for the sigmoidal regulation function from Figure 2, we take $a = 5$, $b = 1$; the protein degradation rate $\delta = 0.05$; the morphogen gradient as the input into the A-gene follows an exponential increase as $M = Id^c$, with $I = 5$, $d = 0.982$, and c, the integer cell number decreasing as c: $32 - 1$. The promoters of the three genes are characterised by the same sigmoidal function. The steady states of the system are calculated from the ordinary differential equations:

$$\dot{A} = \frac{1}{1+\exp(a - bId^c)} - \delta A \tag{1}$$

$$\dot{B} = \frac{1}{1+\exp[a - b(\omega_{AB}A - \omega_{BB}B - \omega_{CB}C)]} - \delta B \tag{2}$$

$$\dot{C} = \frac{1}{1+\exp[a - b(\omega_{AC}A - \omega_{BC}B - \omega_{CC}C)]} - \delta C \tag{3}$$

The strength of the interactions are considered $|\omega_{XY}| \in [0, 10]$, and the initial condition, $(A, B, C) = (0.1, 0.1, 0.1)$. The exhaustive search of stripe-generating parameters is performed under a sampling of $\Delta\omega = 0.2$. Sampling under a finer resolution maintains the results obtained, including the quantitative measures of the fraction of parametric volume (**Supporting Information**, Fig. S11). We verified in such comparisons that there is no translation of the functional values, such that a ratio of 1 implies a complete superposition. Similarly, in a comparison between a level-4 and a level-5 network, the common space to be compared is 4D.

The definition of stripe in the numerical simulations considers the existence of a peak whose left and right border are set by a value of $B_{Low} = 10\%$ of the maximum

value possible for the protein expression. This maximum expression is $B_{Max} = 1/d$, the inverse of the degradation rate.

1. Hartwell, L. H., Hopfield, J. J., Leibler, S. & Murray, A. W. From molecular to modular cell biology. *Nature* **402**, 47–52 (1999).
2. Wagner, G. P., Pavlicev, M. & Cheverud, J. M. The road to modularity. *Nat Rev Genet* **8**, 921–931 (2007).
3. Milo, R. *et al*. Network motifs: simple building blocks of complex networks. *Science* **298**, 824–827 (2002).
4. Ingram, P. J., Stumpf, M. P. H. & Stark, J. Network motifs: structure does not determine function. *BMC Genomics* **7**, e108 (2006).
5. Alexander, R. P., Kim, P. M., Emonet, T. & Gerstein, M. B. Understanding modularity in molecular networks requires dynamics. *Sci Signal* **2**, e44 (2009).
6. Davidson, E. H. Emerging properties of animal gene regulatory networks. *Nature* **468**, 911–920 (2010).
7. Alon, U. Network motifs: theory and experimental approaches. *Nat Rev Genet* **8**, 450–461 (2007).
8. Tyson, J. J. & Novák, B. Functional motifs in biochemical reaction networks. *Annu Rev Phys Chem* **61**, 219–240 (2010).
9. Nandagopal, N. & Elowitz, M. B. Synthetic biology: integrated gene circuits. *Science* **333**, 1244–1248 (2011).
10. Papatsenko, D. Stripe formation in the early fly embryo: principles, models, and networks. *Bioessays* **31**, 1172–1180 (2009).
11. Wolpert, L. One hundred years of positional information. *Trends Genet* **12**, 359–364 (1996).
12. Ashe, H. L. & Briscoe, J. The interpretation of morphogen gradients. *Development* **133**, 385–394 (2006).
13. Jaeger, J. *et al*. Dynamical analysis of regulatory interactions in the gap gene system of Drosophila melanogaster. *Genetics* **167**, 1721–1737 (2004).
14. Reeves, G. T. & Stathopoulos, A. Graded dorsal and differential gene regulation in the Drosophila embryo. *Cold Spring Harb Perspect Biol* **1**, e000836 (2009).
15. Green, J. Morphogen Gradients, Positional Information, and Xenopus: Interplay of Theory and Experiment. *Dev Dyn* **225**, 392–408 (2002).
16. Dessaud, E., McMahon, A. P. & Briscoe, J. Pattern formation in the vertebrate neural tube: a sonic hedgehog morphogen-regulated transcriptional network. *Development* **135**, 2489–2503 (2008).
17. Jaeger, J. *et al*. Dynamic control of positional information in the early Drosophila embryo. *Nature* **430**, 368–371 (2004).
18. Nahmad, M. & Lander, A. D. Spatiotemporal mechanisms of morphogen gradient interpretation. *Curr Opin Genet Dev* **21**, 726–731 (2011).
19. Balaskas, N. *et al*. Gene regulatory logic for reading the Sonic Hedgehog signaling gradient in the vertebrate neural tube. *Cell* **148**, 273–284 (2012).
20. Peter, I. S., Faure, E. & Davidson, E. H. Predictive computation of genomic logic processing functions in embryonic development. *Proc Natl Acad Sci U S A* **111**, 906–913 (2012).
21. Kim, M.-S., Kim, J.-R., Kim, D., Lander, A. D. & Cho, K.-H. Spatiotemporal network motif reveals the biological traits of developmental gene regulatory networks in Drosophila melanogaster. *BMC Syst Biol* **6**, e31 (2012).
22. Ishihara, S. & Shibata, T. Mutual interaction in network motifs robustly sharpens gene expression in developmental processes. *J Theor Biol* **252**, 131–144 (2008).
23. Kaplan, S., Bren, A., Dekel, E. & Alon, U. The incoherent feed-forward loop can generate non-monotonic input functions for genes. *Mol Syst Biol* **4**, e203 (2008).
24. Rodrigo, G. & Elena, S. F. Structural Discrimination of Robustness in Transcriptional Feedforward Loops for Pattern Formation. *PLoS One* **6**, e16904 (2011).
25. Basu, S., Gerchman, Y., Collins, C. H., Arnold, F. H. & Weiss, R. A synthetic multicellular system for programmed pattern formation. *Nature* **434**, 1130–1134 (2005).
26. Saka, Y. & Smith, J. C. A mechanism for the sharp transition of morphogen gradient interpretation in Xenopus. *BMC Dev Biol* **7**, e47 (2007).
27. Greber, D. & Fussenegger, M. An engineered mammalian band-pass network. *Nucleic Acids Res* **38**, e174 (2010).
28. Cotterell, J. & Sharpe, J. An atlas of gene regulatory networks reveals multiple three-gene mechanisms for interpreting morphogen gradients. *Mol Syst Biol* **6**, 425 (2010).
29. Irvine, K. D. & Rauskolb, C. Boundaries in development: formation and function. *Annu Rev Cell Dev Biol* **17**, 189–214 (2001).
30. Lewis, J., Slack, J. M. & Wolpert, L. Thresholds in development. *J Theor Biol* **65**, 579–590 (1977).
31. Mitrophanov, A. Y. & Groisman, E. A. Positive feedback in cellular control systems. *Bioessays* **30**, 542–555 (2008).
32. Seo, C. H., Kim, J.-R., Kim, M.-S. & Cho, K.-H. Hub genes with positive feedbacks function as master switches in developmental gene regulatory networks. *Bioinformatics* **25**, 1898–1904 (2009).
33. Mjolsness, E., Sharp, D. H. & Reinitz, J. A connectionist model of development. *J Theor Biol* **152**, 429–453 (1991).
34. Reinitz, J., Mjolsness, E. & Sharp, D. H. Model for cooperative control of positional information in Drosophila by *bicoid* and maternal *hunchback*. *J Exp Zool* **271**, 47–56 (1995).
35. Solé, R. V., Salazar-Ciudad, I. & Garcia-Fernandez, J. Common pattern formation, modularity and phase transitions in a gene network model of morphogenesis. *Physica A* **305**, 640–654 (2002).
36. Manu *et al*. Canalization of gene expression and domain shifts in the Drosophila blastoderm by dynamical attractors. *PLoS Comput Biol* **5**, e1000303 (2009).
37. Zhou, J. X. & Huang, S. Understanding gene circuits at cell-fate branch points for rational cell reprogramming. *Trends Genet* **27**, 55–62 (2011).
38. Ishihara, S., Fujimoto, K. & Shibata, T. Cross talking of network motifs in gene regulation that generates temporal pulses and spatial stripes. *Genes Cells* **10**, 1025–1038 (2005).
39. Purnick, P. E. M. & Weiss, R. The second wave of synthetic biology: from modules to systems. *Nat Rev Mol Cell Biol* **10**, 410–422 (2009).
40. Parter, M., Kashtan, N. & Alon, U. Environmental variability and modularity of bacterial metabolic networks. *BMC Evol Biol* **7**, e169 (2007).
41. Widder, S., Solé, R. & Macía, J. Evolvability of feed-forward loop architecture biases its abundance in transcription networks. *BMC Syst Biol* **6**, e7 (2012).
42. Goldbeter, A., Gonze, D. & Pourquié, O. Sharp developmental thresholds defined through bistability by antagonistic gradients of retinoic acid and FGF signaling. *Dev Dyn* **236**, 1495–1508 (2007).
43. Graham, T. G. W., Tabei, S. M. A., Dinner, A. R. & Rebay, I. Modeling bistable cell-fate choices in the Drosophila eye: qualitative and quantitative perspectives. *Development* **137**, 2265–2278 (2010).
44. Sokolowski, T. R., Erdmann, T. & ten Wolde, P. R. Mutual Repression Enhances the Steepness and Precision of Gene Expression Boundaries. *PLoS Comput Biol* **8**, e1002654 (2012).
45. Zhang, L. *et al*. Noise drives sharpening of gene expression boundaries in the zebrafish hindbrain. *Mol Syst Biol* **8**, e613 (2012).
46. Kim, D., Kwon, Y.-K. & Cho, K.-H. The biphasic behavior of incoherent feed-forward loops in biomolecular regulatory networks. *Bioessays* **30**, 1204–1211 (2008).
47. Macía, J., Widder, S. & Solé, R. Specialized or flexible feed-forward loop motifs: a question of topology. *BMC Syst Biol* **3**, e84 (2009).
48. Goentoro, L., Shoval, O., Kirschner, M. W. & Alon, U. The incoherent feedforward loop can provide fold-change detection in gene regulation. *Mol Cell* **36**, 894–899 (2009).
49. Walczak, A. M., Tkacik, G. & Bialek, W. Optimizing information flow in small genetic networks. II. Feed-forward interactions. *Phys Rev E Stat Nonlin Soft Matter Phys* **81**, 041905 (2010).
50. Osella, M., Bosia, C., Corá, D. & Caselle, M. The role of incoherent microRNA-mediated feedforward loops in noise buffering. *PLoS Comput Biol* **7**, e1001101 (2011).
51. Mangan, S. & Alon, U. Structure and function of the feed-forward loop network motif. *Proc Natl Acad Sci U S A* **100**, 11980–11985 (2003).
52. Zinzen, R. P. & Papatsenko, D. Enhancer responses to similarly distributed antagonistic gradients in development. *PLoS Comput Biol* **3**, e84 (2007).
53. Zartman, J. J. & Shvartsman, S. Y. Enhancer organization: transistor with a twist or something in a different vein? *Curr Biol* **17**, 1048–1050 (2007).
54. Lembong, J., Yakoby, N. & Shvartsman, S. Y. Pattern formation by dynamically interacting network motifs. *Proc Natl Acad Sci U S A* **106**, 3213–3218 (2009).
55. Lander, A. D. Pattern, growth, and control. *Cell* **144**, 955–969 (2011).
56. Rogers, K. W. & Schier, A. F. Morphogen gradients: from generation to interpretation. *Annu Rev Cell Dev Biol* **27**, 377–407 (2011).
57. Fujimoto, K., Ishihara, S. & Kaneko, K. Network evolution of body plans. *PLoS ONE* **3**, e2772 (2008).
58. Kim, M.-S., Kim, J.-R. & Cho, K.-H. Dynamic network rewiring determines temporal regulatory functions in Drosophila melanogaster development processes. *BioEssays* **32**, 505–513 (2010).
59. Cağatay, T., Turcotte, M., Elowitz, M. B., Garcia-Ojalvo, J. & Süel, G. M. Architecture-dependent noise discriminates functionally analogous differentiation circuits. *Cell* **139**, 512–522 (2009).
60. Kaneko, K. Evolution of robustness to noise and mutation in gene expression dynamics. *PLoS One* **2**, e434 (2007).

Acknowledgments

We thank J. Jaeger, M. Louis, A. Gomez an R. Alves for critical discussions.

Author contributions

J.S. conceived and supervised the study. A.M. performed the calculations and wrote the manuscript. R.S. designed the figures. J.C. contributed to the discussion of the results. All authors participated in the critical revision of the manuscript.

Additional information

Supplementary information accompanies this paper at http://www.nature.com/scientificreports

Competing financial interests: The authors declare no competing financial interests.

How to cite this article: Munteanu, A., Cotterell, J., Solé, R.V. & Sharpe, J. Design principles of stripe-forming motifs: the role of positive feedback. *Sci. Rep.* **4**, 5003; DOI:10.1038/srep05003 (2014).